Chapter 1: Introduction to DNA-Mediated Electrochemistry

Adapted from: Gorodetsky, A. A., Buzzeo, M., Barton, J. K. (2008) *Bioconjugate Chem. ASAP.*

1.1 Introduction

Since the elucidation of the double helical structure of DNA, scientists have been fascinated by the possibility that the stacked aromatic base pairs of the duplex may promote charge transport (CT) over significant distances (1, 2). Consequently, the nature of the conductive properties of duplex DNA has attracted substantial interest (3–7). Over the past two decades, a wide-ranging collection of experiments has both revealed the fundamental details of DNA-mediated CT and illustrated its potential for sensing applications.

Initial solution experiments featured photoinduced DNA-mediated CT between well-defined donor and acceptor sites (8, 9). While long-range CT was shown to yield oxidative damage in DNA up to 200 Å away from the bound oxidant (10, 11), DNA CT was also found to be exquisitely sensitive to not only the integrity of the base pair stack (9, 12) but also the coupling of the donors and acceptors with the DNA (13). Indeed, this sensitivity prompted both the consideration of biological roles for DNA CT (14) and the construction of electrochemical DNA-based sensors for mutations, base lesions, and protein-binding (15).

Electrochemical techniques provide a particularly convenient means for the study of heterogeneous electron transfer at solid surfaces (16). Typically, redox-active molecules are modified with thiol-terminated alkyl chains and self-assembled as well-ordered monolayers on metallic surfaces (17). Under an applied potential, electrons or holes are then transferred to pendant, redox-active head groups with the rates and yield of charge transfer (as measured electrochemically) providing information on the structure of

the thiol-terminated linker. In our laboratory, we have extended this methodology to the study and application of DNA-modified surfaces where charge transfer is *mediated* by the DNA monolayers, which are self-assembled onto conductive substrates.

Prior to a discussion of the applications of this methodology, it is important to have a clear understanding of the architecture of DNA-modified surfaces. To facilitate monolayer formation, duplex DNA is modified at the 5' end of a single strand with a linker (an alkanethiol in the case of gold and pyrene in the case of graphite), which allows the DNA molecules to interact with the electrode surface (Figure 1.1). Electrodes are then incubated with modified duplexes and an organized monolayer is allowed to self-assemble. A redox-active molecule is introduced either by exposure to a solution or through covalent attachment to the 5' terminus of the single strand lacking the linker. Subsequent addition of an inert backfilling agent, such as mercaptohexanol, promotes the removal of non-specifically adsorbed duplexes and single strands. The uniformity and reliability of this structure effectively enables the duplexes to serve as an extension of the active electrode surface, thus allowing DNA-bound, redox-active molecules to be reduced via the π-stack. Moreover, since the electrochemistry of the probe is remarkably sensitive to the integrity of the base pair stack, any perturbation of the base pair stack, which intervenes between the probe and the surface, dramatically attenuates the electrochemical yield of CT.

It is noteworthy that the charge transport properties of DNA monolayers are not simply of utility in the context of electrochemistry, as illustrated in Chapter 2. Previous experiments, which found a staggering range of value for the conductivity of DNA,

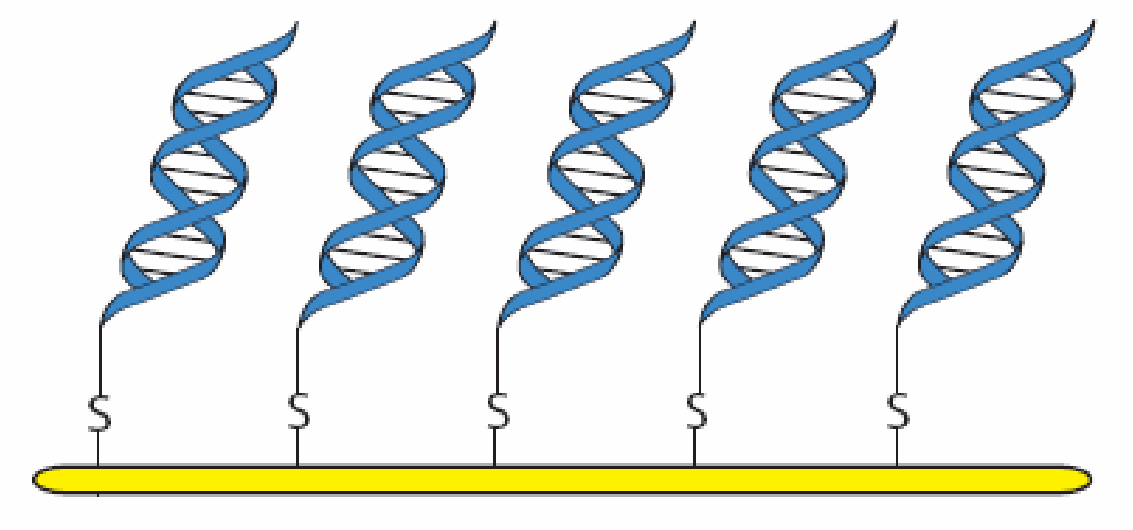

Figure 1.1: Schematic illustration of DNA duplexes in a close-packed monolayer which is immobilized on gold via an alkanethiol tether

nonetheless hinted that charge transport in such monolayers was not simply an ensemble property of an aligned film (18–20). Indeed, our more recent experiments, where a single DNA molecule was utilized to bridge a carbon nanotube gap, confirmed that it is the base pair stack of each individual duplex which serves as a conduit for charge transfer (21). In fact, when considered in the context of an electrical circuit, the DNA duplexes and bound redox-active probes can be viewed as transducer elements with extraordinary gain; biochemical binding events such as hybridization are sensitively transduced into electrical signals. This emphasizes the role of DNA as a remarkably unique medium that provides unprecedented opportunities for studies and applications of long-range CT.

The thesis work presented here concerns the development of new techniques and methodologies for the electrochemical monitoring of DNA binding proteins, with a particular emphasis on applications. This encompasses the characterization of alternative surfaces such as graphite, development of new electrochemical probes, explorations of electrical measurements at the micro- and nanoscales, and extensions to multiplexing. Taken together, these developments constitute a firm foundation for novel biosensors which are based on the exquisite sensitivity of DNA-mediated CT to perturbations of the base pair stack.

1.2 Characterization of DNA Monolayers

For proper interpretation of experimental observations, extensive physical characterization of these self-assembled DNA monolayers has been crucial. A gamut of experimental techniques have been utilized for investigating the structure and

characteristics of DNA monolayers on gold including (but not limited to) radioactive labeling (22–25), fluorescence self-interference (26–28), scanning tunneling microscopy (29–31), atomic force microscopy (23, 25, 32–36), scanning electrochemical microscopy (37–39), and surface plasmon resonance (40, 41). When dense DNA monolayers are desired, the monolayers are assembled in the presence of Mg^{2+} to allow for close packing of the duplexes (schematically illustrated in Figure 1.1). Our group, in particular, has focused on surface characterization via radioactive labeling and scanning probe techniques. These investigations have indicated that DNA monolayers adopt an upright orientation and have predictable surface coverages, thereby allowing us to develop a detailed picture of DNA monolayer morphology.

1.2.1 Thiolated-DNA Monolayers on Gold

Radioactive labeling of the duplexes provides a reliable measure of surface coverage for DNA monolayers. In a typical radioactive labeling experiment on gold, the 5' end of the DNA complementary to the thiolated strand is labeled with polynucleotide kinase, and the amount of DNA is quantified directly via scintillation counting after self-assembly. On gold, these measurements indicated surface coverages of ~ 40 pmol/cm^2 for well-packed DNA monolayers self-assembled in the presence of Mg^{2+} (22) and coverages of ~ 12 pmol/cm^2 for loosely-packed DNA monolayers in the absence of Mg^{2+} (23). Interestingly, the well packed monolayer coverages obtained via radioactive labeling correspond to only ~ 75 % of the theoretical coverages of less than 60 pmol/cm^2, with DNA helices packed perpendicular to the surface. This fact supports the notion that the DNA is oriented at an angle with respect to the surface.

While radioactive labeling affords a quantitative measurement of the overall surface coverage, the electronic structure of local areas of a DNA monolayer can be probed via scanning tunneling microscopy (STM), providing atomic level information (29). Indeed, STM allows for the investigation of the electronic properties of DNA as a function of duplex orientation. Therefore, the images obtained yield information on not only the morphology but also the local density of states of the sample. At negative potentials, where the DNA adopts an upright orientation, agglomerates of duplexes are visible because the tip can electronically access the oriented DNA in an effective metal-molecule-metal junction. However, at positive potentials, the DNA is encouraged to lie down and the DNA film is effectively not visible to the STM tip. These data indicated that the DNA duplexes comprising a DNA monolayer aggregate in small hexagonal groups of ~ 10 nm diameter. Furthermore, the inclusion of a mismatch within the monolayer dramatically attenuates communication between the tip and the surface, demonstrating that the STM is accessing the local density of states of the full DNA duplex.

The morphology of self-assembled DNA monolayers can be further explored at the nanometer scale with atomic force microscopy (AFM). These investigations have indicated that 5' tethered films are essentially smooth and featureless within the resolution of the AFM tip with the DNA dispersed in a uniform manner (32). AFM measurements also provide important information about the morphology and depth of the DNA monolayer at various substrate biases. By applying a large downward force to the monolayer with the AFM tip, a bare spot can be uncovered on the DNA-modified surface. Height contrast measurements between this bare spot and the surrounding DNA

monolayer indicate a film depth which ranges from 4.2 to 4.6 nm for 15 mer duplexes at open circuit on gold. In fact, the height of these films can be reversibly modulated from 2 nm (the diameter of the duplex) at positive potentials to 5.5 nm (the full length of the duplex when normal to the surface) at negative potentials (Figure 1.2). These data, in conjunction with the above experiments, indicate that the duplexes adopt an upright orientation at negative potentials and are oriented at a ~ 45 º angle with respect to the surface in the absence of an applied bias (25, 32).

1.2.2 ***Pyrenated-DNA Monolayers on Graphite***

Physical characterization of DNA monolayers on graphite is crucial for the development of this material as an alternative surface for investigations of DNA CT. The preparation and investigation of DNA monolayers on highly oriented pyrolytic graphite (HOPG) is described in Chapter 3; the monolayers are formed in an identical fashion to those on gold, but the DNA is anchored to the surface via a hydrophobic, pyrenated tether (25). Radioactive labeling indicates similar DNA densities on graphite as on gold. In addition, AFM measurements reveal that DNA monolayers on graphite are smooth and featureless with a film depth of 4.4 nm for monolayers consisting of 15 mer duplexes. Taken together, AFM measurements and radioactive labeling studies indicate that well-packed DNA monolayers on graphite are oriented at an angle with respect to the surface and are essentially identical to thiolated DNA monolayers formed on gold.

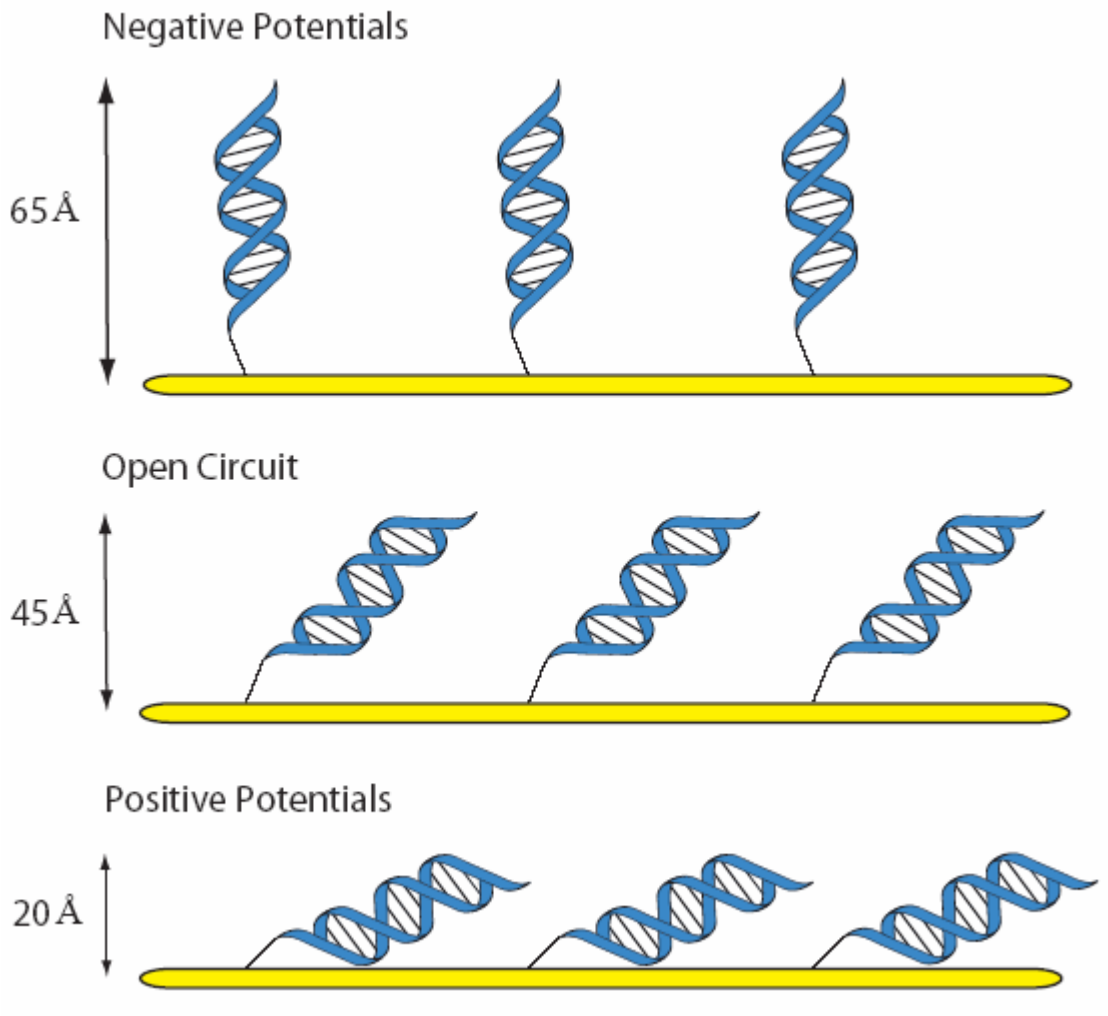

Figure 1.2: Schematic illustration of the modulation of the height of a DNA monolayer at different substrate potentials. At open circuit, imaging studies have shown that duplexes are oriented upright and at a ~ 45º angle relative to the surface. At positive potentials, the polyanionic DNA duplexes are attracted to the surface, while at negative potentials the duplexes are in an upright orientation with the helix axes perpendicular to the electrode surface.

1.3 Electrochemistry of Small Molecules Non-covalently Bound to DNA

Numerous redox-active probes have been utilized for investigations of DNA CT, and, at first glance, many molecules appear adequate for these studies. The large collection of experiments conducted in our laboratory over the past decade, however, has taught us essential lessons regarding the selection of an appropriate redox probe. Three criteria are paramount: the species must (i) be electronically well coupled to the base pair stack, (ii) be reliably linked to the duplex, and (iii) undergo stable reduction or oxidation within a potential window that does not compromise the integrity of the DNA monolayer. Furthermore, in addition to affording insight into the optimum probe design, our systematic studies clearly indicate that no one probe is ideally suited for every experiment. Instead, different markers offer distinct advantages and must be individually evaluated for specific applications.

The behavior of the redox probes employed in our studies do, however, display some common features when monitored electrochemically. When bound to DNA, small molecules appear to act as surface-bound species, as indicated by a linear relationship between the peak current and scan rate. This relationship is not strictly linear for DNA-bound redox proteins, where the proteins are not situated in one fixed position or conformation and thus exhibit a slight diffusive component. Nonetheless, covalent probes bound to DNA typically do not display a square-root-dependence of the peak current on the scan rate that is indicative of free diffusion. In addition, DNA binding typically shifts the redox potential of the probe by 20–50 mV from direct reduction at the bare surface and the voltammetry adopts a skewed shape relative to a classically adsorbed couple; the

reductive and oxidative peaks are separated slightly due to the intervening DNA/alkanethiol spacer. Electrochemical reversibility and stability are also specific to each probe, but they can be interrogated simply by repetitive cycling over the potential window of interest. Taken together, all of these features allow us to distinguish DNA-mediated processes from ones involving direct electrochemistry.

1.3.1 DNA-Mediated Electrochemistry on Gold

Early work on gold employed probes that were not covalently attached to DNA but instead interacted with the base pair stack electrostatically or via intercalation (22). Although the majority of our studies have involved the intercalator methylene blue, we have also studied the interaction between DNA and anionic ferricyanide, cationic ruthenium hexammine, the tris-heteroleptic intercalator $Ir(bpy)(phen)(phi)^{3+}$, and the anti-tumor agent Daunomycin (Figure 1.3). While these non-covalent markers have afforded a significant foundation for the study of DNA-mediated CT, they are intrinsically limited in the mechanistic detail and experimental control they can provide. As a result, latter experiments focused on developing covalently bound probes, specifically those that are electronically well coupled to the base pair stack.

Methylene blue (MB), a well-studied aromatic intercalator that undergoes a $2e^-/1H^+$ reduction in aqueous systems, has served as a workhorse reporter of DNA-mediated processes (22). Figure 1.4 shows a schematic illustration of the reduction of MB at a DNA monolayer; a reversible redox couple is seen with a midpoint potential centered at -10 to -50 mV vs. NHE, shifted by ~ 30 mV from bare gold. The measured peak currents scale linearly with scan rate, indicating that the redox molecule is surface bound, and a combination of electrochemical and spectroscopic measurements give a saturation value

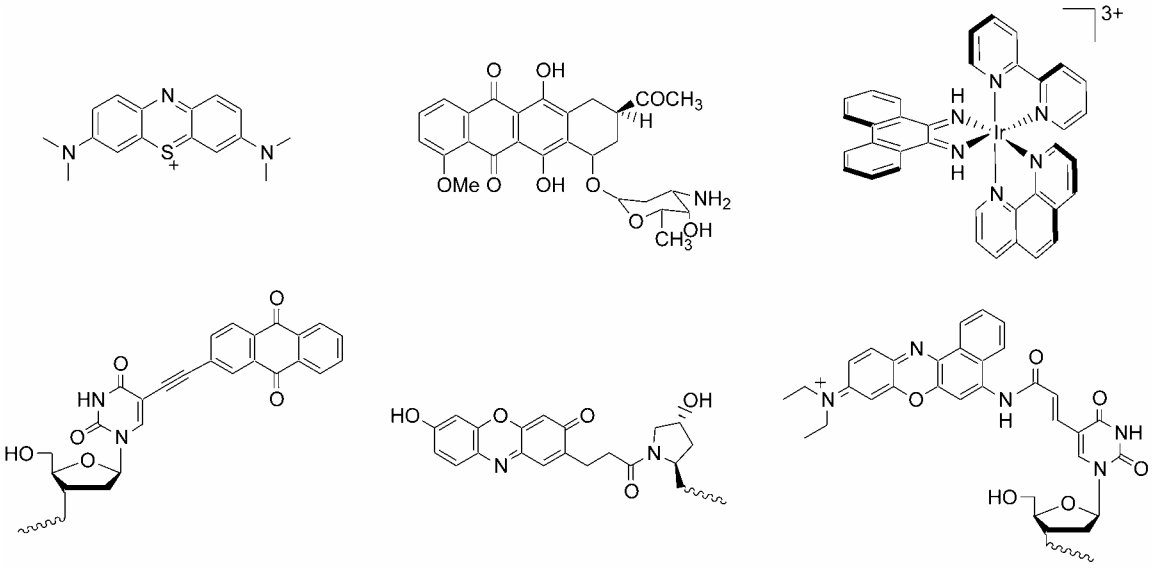

Figure 1.3: Chemical structures of redox-active probes which have been utilized to explore DNA-mediated CT. Non-covalent probes are on the top row (from left to right): Methylene blue, Daunomycin, and Ir(bpy)(phen)(phi)$^{3+}$. Covalent probes are on the bottom row (from left to right): Anthraquinone, Redmond Red, and Nile Blue.

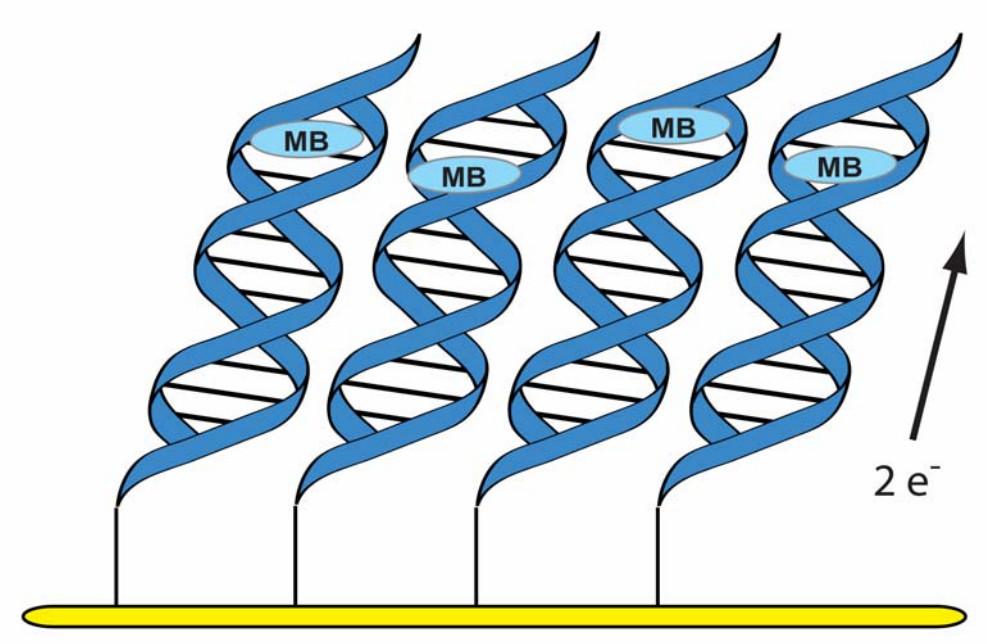

Figure 1.4: Schematic illustration of the reduction of methylene blue (blue) via DNA-mediated CT at a well-packed DNA monolayer. The probe is constrained to intercalate near the top of the monolayer.

of 1.4(2) molecules per duplex at high MB concentrations. This latter finding suggests that, for well-packed monolayers, MB is constrained to the top of the film. Any observed reduction, therefore, can be attributed to a DNA-mediated process, as the surface is inaccessible to the molecule.

To further prove that the reduction of distally bound probes proceeds in a DNA-mediated fashion, the electrochemistry of MB and other small molecules was explored at DNA monolayers containing single base mismatches positioned between the electrode surface and the probe (45). It was theorized that if the DNA base pairs combined to form a continuous, π-stacked conduit for charge transfer, that the disruption of a single base pair, as in a mismatch, could interrupt the CT pathway. The presence of a single base mismatch causes no global change in the duplex structure, and yet, the inclusion of an intervening CA mismatch proved to have a dramatic effect on the efficiency of charge transfer to MB. These results are in excellent agreement with STM studies of matched and mismatched duplexes and with studies of photoinduced DNA CT in solution (9) (*vide supra*). Interestingly, not only could several mismatches be detected but the DNA-mediated chemistry was also found to be independent of sequence context. Furthermore, this exquisite sensitivity to base pair stacking was observed for numerous intercalating (but not groove-binding) probes, supporting the notion that the observed electrochemistry is DNA-mediated and a general characteristic of the DNA.

To increase the sensitivity of mismatch detection and further improve discrimination, MB was coupled to freely diffusing $Fe(CN)_6^{3-}$ in an electrocatalytic cycle (Figure 1.5). In this catalytic process, MB undergoes a two e^- reduction via the base pair

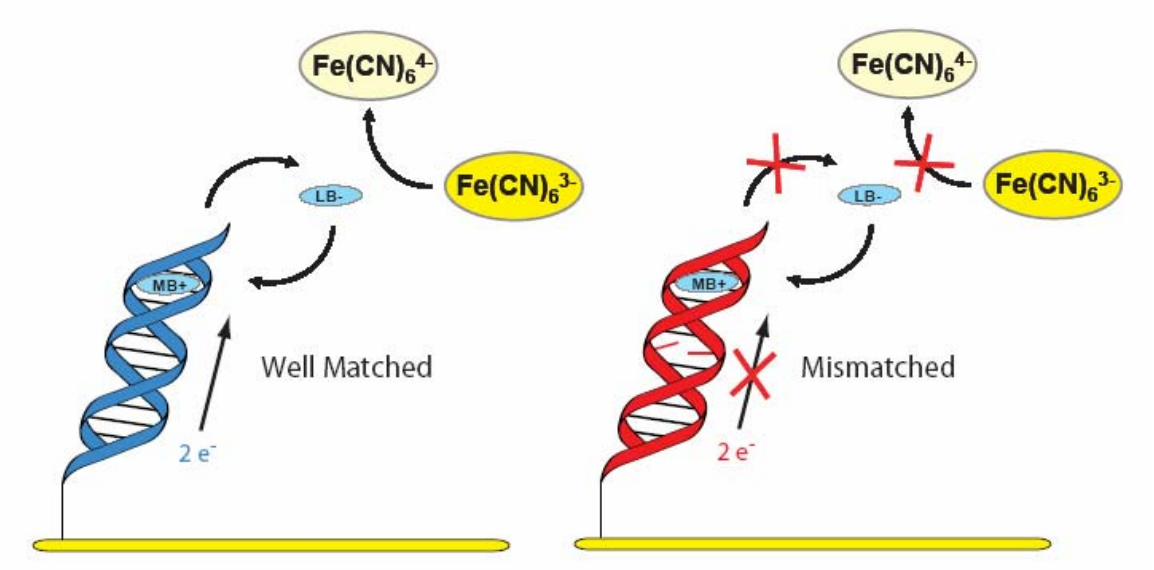

Figure 1.5: Schematic illustration of the methylene blue/ferricyanide electrocatalytic cycle at a DNA monolayer. DNA-bound methylene blue is reduced in a DNA-mediated reaction to leucomethylene blue (LB), which dissociates from the monolayer and is reoxidized by ferricyanide in solution; the reoxidized methylene blue returns to the DNA for another round of DNA-mediated electrochemistry. This electrochemical amplification leads to enhanced discrimination of all single base mismatches in DNA, since the intervening mismatch shuts down the DNA-mediated reaction and thus the electrocatalytic cycle.

stack, and upon reduction to leucomethylene blue, loses some affinity for DNA, thus dissociating from the duplex (45, 46). In turn, the cycle continues when leucomethylene blue is reoxidized by $Fe(CN)_6^{3-}$ in solution, and binds again to DNA for another cycle of DNA-mediated reduction. It should be noted that $Fe(CN)_6^{3-}$ cannot be reduced directly at the negatively charged monolayer owing to repulsion from the polyanionic DNA monolayer. The entire process is effectively governed by the on/off kinetics of the methylene blue/leucomethylene blue redox couple, as confirmed by rotating disk electrode experiments (48). In fact, during the course of a single voltammogram, the DNA is repeatedly sampled, amplifying the absolute signal of MB and increasing the signal attenuation associated with a mismatch.

The detection of all naturally occurring mismatches and nearly all common lesions was achieved with the MB/$Fe(CN)_6^{3-}$ electrocatalytic couple via cyclic voltammetry and chronocoulometry. In addition, low detection limits were demonstrated in a chip-based format, with mismatch discrimination possible at electrodes as small as 30 μm in diameter (46). It should also be noted that the relatively stable GA mismatch could *not* be detected without the aid of the described catalytic cycle, emphasizing the utility of electrocatalysis as an electrochemical tool. Furthermore, even base lesions that cause minor thermodynamic destabilization to the duplex could be detected with electrocatalysis: a systematic investigation revealed that the efficiency of CT was dramatically decreased even by subtle base modifications that altered base structure, steric bulk, or hydrogen bonding (49). Perhaps not surprisingly, modifications with methyl groups that do not participate in hydrogen-bonding had little-to-no effect on the DNA-mediated electrochemistry. The sensitive detection of all single base mismatches

independent of sequence context is remarkable and has proven to be valuable in the application of DNA electrochemistry for the diagnosis of single nucleotide polymorphisms.

1.3.2 DNA-Mediated Electrochemistry on Graphite

To electrochemically characterize HOPG, MB and DM electrochemistry is also explored at self-assembled DNA monolayers on this surface, as described in Chapter 3. The behavior of both intercalators on graphite is quite similar to that on gold, and evidence that the charge transfer is DNA-mediated is provided by the facile detection of the CA and GT mismatches. In addition, as on gold, mismatch discrimination with MB on graphite can be dramatically improved by couple MB to ferricyanide in a catalytic cycle. Notably, as a surface, HOPG provides an attractive alternative since its accessible potential window is no longer limited by the oxidative reduction or desorption of thiols. In fact, the wider potential window afforded by HOPG allows for the study of the voltammetry of $Ru(bpy)_2dppz^{2+}$ and $Os(phen)_2dppz^{2+}$. As expected, the electrochemistry of both intercalators is DNA-mediated.

1.4 DNA-Mediated Electrochemistry of Small Molecules Covalently Bound to DNA

To facilitate the systematic investigation of charge transduction of DNA, it became necessary to employ redox-active probes that are covalently conjugated to the base pair stack. These initial efforts focused on covalently attached daunomycin (DM), which can be site-specifically cross-linked to the exocyclic amine of guanine, forming a covalent bond, as shown in Figure 1.6 (50–52). Most importantly, this allows for

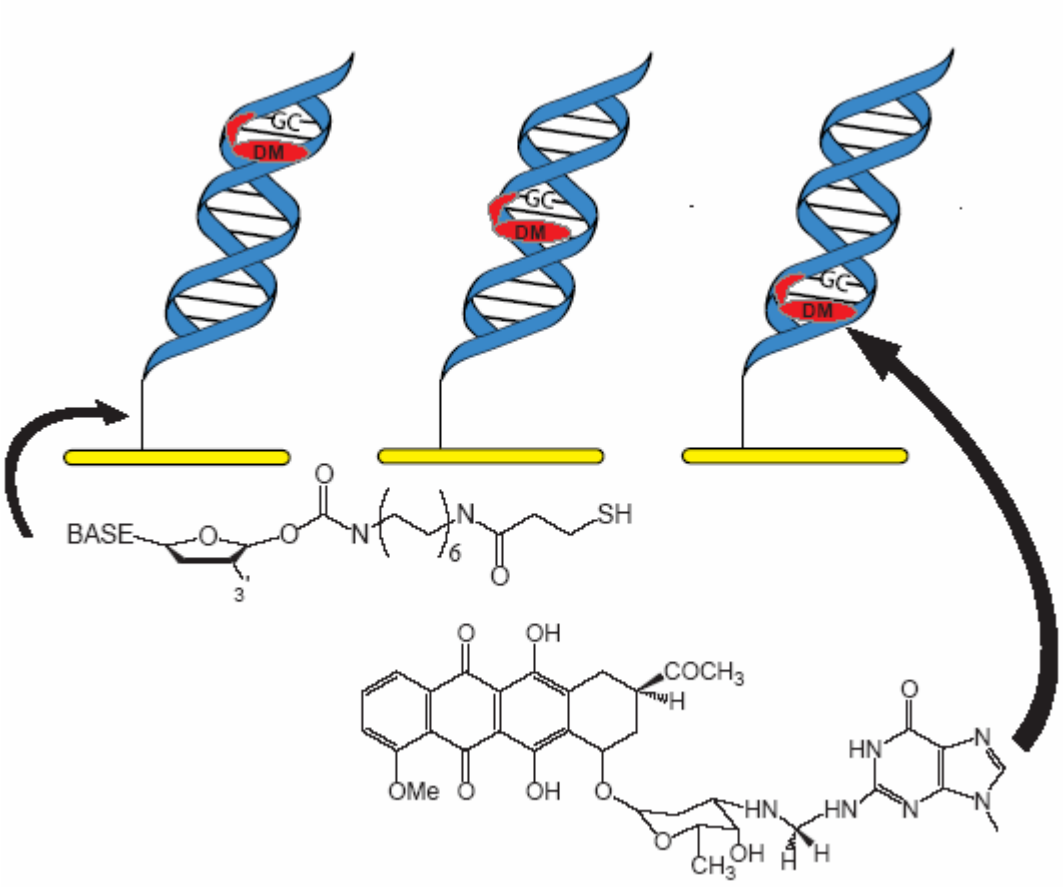

Figure 1.6: A schematic illustration of DNA duplexes with daunomycin covalently cross-linked at various separations from the electrode surface. Also depicted are the DM-guanine cross-link (bottom right) and the thiol-terminated tether which connects the duplex to the electrode surface (bottom left).

controlled placement of the probe within the sequence. Importantly, the covalent attachment of this probe for DNA electrochemistry has made possible several seminal conclusions about DNA-mediated CT involving *ground-state* reactants.

While DM has afforded several key findings, it does possess some inherent limitations. Since functionalization with DM occurs after the synthesis of the DNA, it does necessitate that all guanines other than the one to be linked are replaced by inosine, a close base analogue. For the purpose of electrochemical measurements, this substitution has no influence on the results, but this requirement limits its applicability in protein detection schemes and biosensors. Moreover, the stability of the linkage between DM and DNA is heat sensitive. As a result, we have been focused on developing a new generation of probes based on phenoxazine and anthraquinone cores that can be covalently attached to DNA with synthetic flexibility, display excellent stability, and are electronically well coupled to the base pair stack.

1.4.1 Electrochemistry of Daunomycin

In initial experiments on gold, the separation between the gold surface and DM adduct was varied from 15 Å to 45 Å, and no effect on the yield or rate of electron transfer was observed (50). The inclusion of a mismatch in the intervening DNA, however, completely shuts off the electrochemistry of DM, conclusively demonstrating that CT is DNA-mediated. Subsequently, with DM held in a fixed position in the duplex, the length of the thiolated alkyl tether was varied to probe the effect of tether length on the rate of charge transfer (51). While the yield of CT remained the same regardless of chain length (the number of intervening methylene units was increased from 4 to 9), significantly, the rate of electron transfer decreased with increased tether length with a β_n

of 1.0 per $–CH_2–$ unit, as expected for the variation in coupling with σ-bonded systems. Therefore, CT through the alkyl tether, not through 30 Å of π-stacked DNA, was the rate-limiting step of the DNA-mediated reduction. Taken together, these findings illustrated that the DNA-DM construct behaves as a single redox-active entity with dramatically different rates of CT through the stacked DNA and the σ-bonded alkyl chain.

In a later study, DM was employed to prove that DNA-mediated electrochemistry occurs via the base pair stack and not the sugar-phosphate backbone (52). With two DM moieties crosslinked to guanine residues, voltammograms of duplexes containing a nick in the backbone, a nick and a mismatch, a nick on both strands, and no modifications were compared. Nicks in the phosphate backbone did not attenuate CT, but, consistent with previous results, mismatches significantly attenuated the electrochemistry of DM. Interestingly, Chapter 4 shows that the electrochemistry of thiols incorporated within the sugar-phosphate backbone is DNA-mediated but proceeds at low yield (53). This demonstrates the utility of graphite for the exploration of redox chemistry which is not accessible on gold. In addition, this work reveals that although DNA electrochemistry proceeds through the base pair stack rather than through the sugar-phosphate backbone, it can promote reactions on the DNA backbone.

1.4.2 Electrochemistry of Anthraquinone

Through a variety of experiments conducted both in our laboratory and others, it has become apparent that efficient coupling of the probe to the base stack is critical for efficient DNA CT. Recently, the groups of Saito and Gooding introduced thymines modified with anthraquinone as effective, covalently attached probes of charge transfer at DNA-modified surfaces (54–57). Using this technology, Gooding and coworkers

demonstrated the application of these modified probes to the detection of primer extension reactions (54, 55), and Saito and coworkers demonstrated the photostimulated detection of mismatches with applications to genotyping of single nucleotide polymorphisms (56, 57). However, the low current densities obtained in these studies led us to conduct a comparative study of anthraquinone linked to DNA through conjugated and saturated tethers, as described in Chapter 5 (58). Importantly, we found efficient redox chemistry and mismatch sensitivity for anthraquinone only when linked through an alkyne and not when tethered by an alkyl chain. Thus not only the choice of probe but also how the probe is coupled to the base pair stack are key to effective DNA-mediated CT.

1.4.3 Electrochemistry of Nile Blue and Redmond Red

More recently, we have investigated two phenoxazine-based probes, Redmond Red (RR) and Nile Blue (NB), as covalent reporters of DNA CT (Figure 1,3). Both of these probes can be incorporated into DNA on solid support, have virtually no sequence restrictions, are stable to light/heat, and support DNA-mediated electrochemistry. Accordingly, they are preferable to DM for routine use and high throughput experiments, and the continued development of these probes holds great promise for future protein detection experiments.

As described in Chapter 7, Redmond Red is commercially available as a phosphoramidite, affording facile incorporation into DNA (59). Although this probe is not perfectly coupled into the DNA π-stack, it can be placed opposite an abasic site to provide a more intimate interaction with the DNA and obtain larger electrochemical signals. In addition, the remarkable stability of this probe makes it particularly useful as

an internal standard for the electrochemistry of the iron-sulfur-containing transcription factor SoxR (*vide supra)*.

NB, as described in detail in Chapters 8–10, can be attached to DNA on solid support by reacting its exocylic amine with a carboxy-NHS-ester-thymine, ensuring that NB is connected to the DNA via a partially saturated linkage (60). Such a linkage affords relatively large electrochemical signals and is similar to the one described by Gooding and coworkers for anthraquinone (54, 55). Furthermore, the electrochemical signal from NB can be amplified via electrocatalysis with oxygen and ferricyanide. This catalytic activity facilitates the characterization of NB-modified DNA monolayers with scanning electrochemical microscopy (SECM) in Chapter 8, affording great insight into the morphology of probe modified films. Finally, as an added benefit, NB indicates its own degradation through the appearance of a new redox signature. All of these features make NB the probe of choice for protein detection experiments at both small scales (Chapter 9) and in a multiplexed format (Chapter 10).

1.5 Electrochemical Monitoring of Protein/DNA Interactions

Self-assembled DNA monolayers provide especially convenient platforms for electrical monitoring of protein/DNA interactions. These interactions play crucial roles in many cellular processes, such as transcription, repair, and replication. In particular, the association of transcription factors with DNA is an important area for exploration in proteomics and genomics; it is these interactions that control the developmental and regulatory responses of the cell, often in a complicated fashion. Therefore, the

development of convenient and inexpensive methodologies for monitoring protein-DNA interactions remains of critical importance.

In a typical experiment, a loosely packed DNA monolayer is self-assembled in the absence of magnesium, with or without a covalently appended probe, and the surface is backfilled (Figure 1.7). Such sparse DNA films are necessary for improved accessibility of proteins; prior to backfilling, they possess a distinct "island" morphology since the DNA has room to lie flat on the gold surface in the absence of an applied potential (23). However, monolayers backfilled with a short chain alkanethiol such as mercaptohexanol have been demonstrated to adopt an upright orientation relative to the gold surface even at open circuit (35, 36). This well-defined morphology is a crucial for accurate sequence-specific detection of DNA binding proteins.

After self-assembly and backfilling, voltammetry of the DNA-modified electrode is recorded in the absence and presence of protein (Figure 1.7). Detection of protein binding can be achieved in two ways: 1) proteins that perturb the base pair stack will attenuate the yield of DNA CT to a distally-bound electroactive probe such as DM, and 2) proteins featuring a redox-active cofactor such as an iron-sulfur cluster will cause the appearance of a new DNA-dependent electrochemical signal. These experiments have greatly benefited from the development of covalently attached probes (*vide supra)* which have allowed for conclusive quantification of the yield of DNA CT before and after protein binding. Furthermore, such electrochemical assays are general and based on exquisitely sensitive DNA-mediated electrochemistry, so a wide range of protein/DNA interactions and binding motifs can be sequence-specifically interrogated in real time.

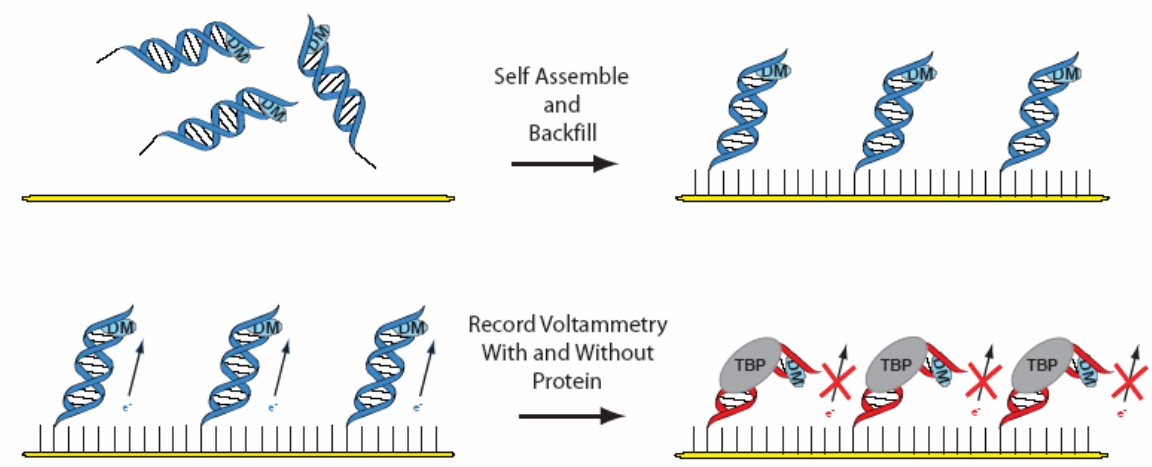

Figure 1.7: Illustration of the fabrication of DNA monolayers on gold and the subsequent electrochemical analysis of protein binding. First, loosely packed DNA monolayers are formed and the surface is backfilled with mercaptohexanol for passivation. In the absence of protein, DNA-mediated redox chemistry to the DNA-bound probe is observed. Binding of a protein that interrupts the base pair stack also interrupts the DNA-mediated redox chemistry, leading to attenuation of the redox signal.

Previous studies at DNA-DM monolayers demonstrated that protein-induced distortions of the base pair stack could be easily detected (23). The perturbations included DNA bending by the TATA-binding protein transcription factor (TBP), base flipping by the *Hha I* methyltransferase (M.Hha I) and uracil deglycosylase (UDG), and cutting by the *Pvu II* restriction enzyme (R.Pvu II). These proteins were chosen for detection experiments since they had all been extensively characterized from a biochemical standpoint. These early efforts hinted at the potential of assays based on DNA CT for the high throughput, multiplexed electrical monitoring of numerous DNA binding proteins on a single chip.

1.5.1 Detection of Base Flipping Enzymes

The electrical detection of methyltransferases, base flipping enzymes which catalyze the transfer of a methyl group from S-adenosylmethionine to adenine or cytosine, is particularly noteworthy. Establishing a base flipping mechanism was historically quite difficult, usually requiring a crystal structure, but the electrical detection of base flipping using DNA electrochemistry has been found to be a sensitive, rapid, and attractive method for such characterization. While methyl substitution does not appreciably perturb the base pair stack, methyltransferases, in carrying out the base flip, significantly attenuate DNA-mediated CT. Based upon this attenuation, we have conducted a detailed exploration of base flipping by *Hha*I methyltransferase upon binding to its cognate sequences (23).

At a surface featuring a DNA-DM monolayer, for example, the addition of M.*Hha*I disrupts the integrity of the base pair stack with a concomitant decrease in the DM redox signal. From the crystal structure of the protein/DNA complex, it is apparent

that upon base flipping the internal cytosine of the recognition sequence 5'-GCGC-3', M.*Hha*I also intercalates the non-aromatic residue Gln 237 into the base pair stack, filling the space occupied by the flipped out cytosine and interrupting π-stacking within the duplex. With this in mind, electrochemistry experiments were conducted with a Q237W mutant enzyme, since it was expected that the mutant protein would insert the aromatic tryptophan residue into the π-stack upon base flipping, leading to little signal loss. Indeed, minimal attenuation of the DM signal upon binding the mutant protein was observed. Moreover, to establish that the lack of attenuation was the result of restoration of the π-stack and not simply poor DNA binding by the mutant, we also examined binding of both wild type and mutant M.*Hha*I to a DNA-DM monolayer containing an abasic site at the position of what would be the flipped out cytosine. On this DNA-DM monolayer, the DM redox signal is only weakly detected both in the absence of protein and in the presence of wild type M.*Hha*I, owing to the poor stacking of the duplex with an intervening abasic site. Nonetheless, in the presence of the Q237W mutant, the DM redox signal is restored. This enhanced signal for DM on binding the mutant reflects insertion of the tryptophan from the mutant protein within the base pair stack, so as to restore proper stacking in the DNA-DM duplex. Hence DNA-binding proteins are seen to modulate DNA CT both positively and negatively, depending upon how they affect the conformation of the DNA.

1.5.2 Detection of Transcription Factors that Distort DNA

Our early studies at DNA-DM monolayers demonstrated that we could easily detect TATA-binding protein (TBP), a transcription factor that bends duplex DNA by ~ 90º upon binding (23). The addition of TBP to a DNA-modified surface results in distortion of the DNA and lowers the yield of DNA CT (Figure 1.7). Consequently, this

transcription factor was chosen as a model system because of its central role in the eukaryotic/prokaryotic transcription machinery, excellent stability, simple 5'-TATA-3' binding site, and well-known structure.

In Chapter 8, the detection of TBP with a scanning probe technique is demonstrated (61). This assay exploits the interruption of a DNA-mediated, bimolecular reaction between DNA-bound NB and ferricyanide, which is generated at the SECM tip. The SECM facilitates the exploration of the morphology of NB-modified DNA monolayers in the presence and absence of proteins which do not bind DNA, such as BSA, and proteins which distort the DNA, such as TBP. In fact, attomoles of TBP, as estimated from the footprint of the SECM tip, are detected only at DNA monolayers which feature the 5'-TATA-3' binding site.

The detection of TBP due to interruption of DNA CT at DNA-modified microelectrodes is described in Chapter 9 (60). At DNA monolayers modified with Nile Blue, TBP can be readily detected at both the macro- and microscales. However, microelectrodes allow for the rapid detection of nanomolar concentrations of this transcription factor even from complicated mixtures containing bovine serum albumin, EndonucleaseIII, or Bam HI methyltransferase.

The sequence-specific detection of TBP from a cell lysate is explored in Chapter 10 via a multiplexed format. The manufacture and individual addressing of multiple electrodes on a single chip affords high throughput experiments and excellent statistics. The detection of TBP is accomplished in two ways: 1) a cell lysate solution is intentionally supplemented with TBP and 2) the transcription factor is overproduced in mouse epithelial cells through treatment with epidermal growth factor. In both cases,

highly accurate detection can be achieved, emphasizing the potential of this methodology for rapid electrical detection of numerous DNA binding proteins from complicated, real - world mixtures.

1.5.3 Electrical Monitoring of Photolyase in Real Time

Another advantage of monitoring protein binding to DNA electrically comes from the fact that this technique allows for the sensitive detection of events in real time; this is best exemplified by the electrical monitoring of thymine dimer repair by photolyase (62). Photolyase is a repair enzyme from *E. coli* containing a flavin cofactor that binds pyrimidine dimers in duplex DNA and repairs them, upon photoactivation, in a reaction involving electron transfer from the reduced flavin cofactor to the dimer flipped out of the DNA duplex by the enzyme. Importantly, in monitoring photolyase reactions electrochemically on DNA monolayers, an externally bound DM redox probe was not utilized; the redox signal of the flavin cofactor, which is intimately associated with the DNA, was monitored instead.

Upon binding of photolyase to a DNA monolayer containing the thymine dimer, a weak redox signal arising at 40 mV versus NHE was first observed. Through control studies with apoprotein and a mutant, this redox signal was assigned to the flavin, and its small size was attributed to poor coupling with the DNA, owing to the intervening destacked thymine dimer. The repair reaction was subsequently carried out by illuminating the electrode surface. With irradiation, an increase of almost an order of magnitude in the integrated flavin signal was observed, and repair of the thymine dimer was confirmed via HPLC analysis. Thus, the repair of the thymine dimer by photolyase was monitored *in real time*, as a function of irradiation; as the photolyase repairs the

thymine dimer, the base pair stack is restored, the flavin cofactor becomes well coupled into the base stack, and its signal is enhanced (Figure 1.8). Subsequently, it was observed that once the DNA is repaired, the protein dissociates from the monolayer, and the intensity of the signal is diminished. Overall, the photolyase experiments illustrated not only how DNA electrochemistry could be used to assess DNA conformational changes associated with protein binding, but also the utility of DNA electrochemistry for measuring the redox potentials of DNA-binding proteins in their biologically relevant forms.

1.5.4 Electrochemistry of Repair Enzymes Containing Iron Sulfur Clusters

DNA electrochemistry has also been more generally applied in assessing the redox characteristics of other DNA-binding proteins in their *active, DNA-bound* form. An illustrative example is found in the characterization of the redox chemistry associated with two base excision repair (BER) enzymes: MutY, a glycosylase that excises adenine from 8-oxoguanine:adenine mispairs, and Endonuclease III, a glycosylase that targets oxidized pyrimidines (63–70). Crystal structures of these enzymes indicated that they both contain an iron-sulfur cluster with the C-X_6-C-X_2-C-X_5-C motif in close proximity to the DNA backbone (64–67). This Fe_4S_4 motif, moreover, is conserved in base excision repair proteins from bacteria to man. Interestingly, in MutY, this cluster is not necessary for protein folding or stability but is crucial for DNA binding and *in vivo* activity (68). EPR experiments have demonstrated that the cluster is in its $[4Fe\text{-}4S]^{2+}$ form when isolated from the cell, but the protein cannot be reduced within a physiologically relevant window nor oxidized by ferricyanide without degradation

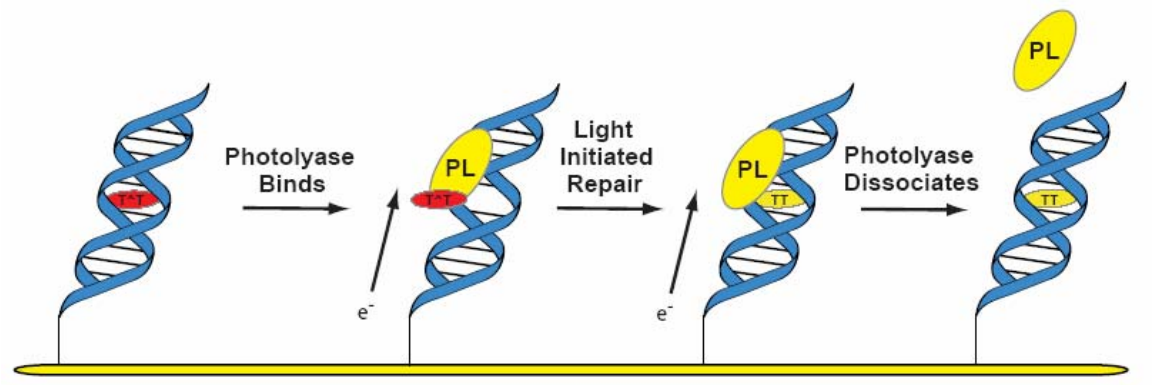

Figure 1.8: Schematic illustration of the electrochemical monitoring of the repair of thymine dimers in a DNA monolayer by photolyase. In the absence of photolyase, no signal is observed, but when the protein is added, a weak signal is observed due to binding of the T^T dimer. Control studies show that the signal corresponds to the flavin bound within the photolyase. Upon irradiation, the thymine dimer is repaired, the integrity of the base pair stack is restored, and the signal grows in intensity. Finally, because the protein has a lower affinity for undamaged DNA, it dissociates, leading to the slow loss of the protein redox signature.

(69, 70). However, these studies, which suggested a lack of redox activity associated with the reactivity of the proteins, were conducted in the absence of DNA. Significantly, we found that EndoIII and MutY display stable, quasi-reversible signals with potentials of ~ 90 mV versus NHE (71, 72), at DNA-modified and backfilled surfaces, and importantly, these signals were not observed at surfaces backfilled with mercaptohexanol but lacking DNA. Furthermore, weak signals were found on surfaces modified with DNA duplexes containing an abasic site, demonstrating that the observed redox processes for the proteins are DNA-mediated.

As illustrated in Chapter 6, experiments performed on DNA-modified HOPG allow for the direct comparison of the electrochemistry of EndoIII in the presence and absence of DNA (73). Qualitatively similar results are obtained in the presence of DNA on gold and HOPG. Due to its extended potential window, however, graphite allows for the study of the electrochemistry of EndoIII also in the absence of DNA, a measurement made impossible by the potential window limit on gold. The ability to measure the redox potential of both free and bound EndoIII on the same surface demonstrates that binding to DNA not only stabilizes the cluster but also shifts its redox potential.

1.5.5 Electrochemistry of an Iron Sulfur Transcription Factor Bound to DNA

SoxR is a 17 kDa transcription factor that binds DNA as a dimer with a [2Fe-2S] cluster in each monomer (59, 74–76). The loss of the cluster does not affect protein folding, DNA binding, or promoter affinity, but oxidation of the cluster triggers the transcription of SoxS and the subsequent expression of over 100 other genes responsible for the oxidative stress response in bacteria. Interestingly, the redox potential of this cluster in the absence of DNA was determined as -290 mV vs. NHE. Importantly, this

measurement of the potential of SoxR led to a conundrum: given the reducing environment of the cell, the cluster would always be in its oxidized form, thereby making SoxR essentially constituitively activated *in vivo*. How does the cell keep this protein reduced and transcriptionally silent unless required?

Since DNA-modified surfaces allow us to determine the redox potential of proteins in their DNA-bound forms, we explore the electrochemistry of the SoxR transcription factor on DNA-modified HOPG in Chapter 7. Such an exploration is particularly relevant given that significant structural differences were recently found between the free (low energy) and DNA-bound (high energy) forms of SoxR (76). In addition, to facilitate these experiments, self-assembled DNA monolayers are prepared on graphite with an appended redox-active probe, Redmond Red (59). Redmond Red provides a convenient internal reference for the voltammetry of the SoxR [2Fe-2S] cluster. Therefore, the redox potential of SoxR is conclusively determined in its physiologically relevant DNA-bound form, shedding light on how the cell regulates the activity of this protein.

These data further underscore the importance of characterizing the redox chemistry of DNA-binding proteins in their biologically relevant, DNA-bound forms. Base excision repair enzymes and transcription factors both represent an interesting target for study, given the ubiquity of the iron-sulfur clusters in these enzymes with no apparent function. Importantly, these are only two examples, and other DNA-binding enzymes that contain a potential redox cofactor may also take advantage of this chemistry. Electrochemistry at self-assembled DNA monolayers thus provides a first assay to

characterize redox chemistry associated with DNA-binding, which may have relevance within the cell.

1.6 Conclusion

The intrinsic ability of DNA to conduct charge along its base pair stack, and the remarkable sensitivity of this chemistry to the integrity of the DNA duplex has been an intriguing topic of study for over two decades. A combination of detailed structural characterization and careful experimental design has allowed the investigation of this chemistry on DNA-modified surfaces. Through a host of electrochemical studies, we have not only uncovered several fundamental properties of this chemistry but have also demonstrated its potential use in a variety of biosensing and biochemical applications.

DNA-modified surfaces offer an ideal platform on which to investigate CT. Structural studies have provided information on the morphology of these self-assembled monolayers, which are found to orient themselves upright and away from the surface, thereby creating an accessible conduit for the transport of charge. We have previously employed several different redox-active, DNA-bound molecules to serve as sensitive reporters of this process. While earlier work largely involved non-covalent intercalating moieties, subsequent studies have taken advantage of the precise control and improved electronic coupling afforded by covalent attachment. In all cases, DNA-mediated CT displays an exquisite sensitivity to the stacking of the base pairs that intervene between the electrode surface and the pendant probe, allowing for the electrochemical discrimination of single base mismatches, lesions, and conformational perturbations.

Finally, due to the possible DNA conformational changes and redox chemistry associated with protein binding, we have also been able to demonstrate the sensitive detection of protein/DNA interactions.

In this thesis, we build upon these previous explorations of DNA CT. In Chapter 2, we demonstrate the single molecule conductivity of DNA, and its applications to the detection of protein binding. DNA monolayers on HOPG are introduced in Chapters 3–7. New covalent probes of DNA CT are explored in Chapters 5, 7, and 8–10. The electrochemistry of proteins containing redox active cofactors is described in Chapters 6 and 7. In addition, the detection of transcription factors that perturb the base pair stack at self-assembled DNA monolayers is explored in Chapters 8–10. Taken together, these studies highlight even further the utility of DNA monolayers for the exploration of DNA CT.

Much remains to be discovered with regard to the scope and fundamentals of this process. Can we harness this chemistry in the construction of highly sensitive nanoscale devices to detect not only proteins but also RNA in real time in a multiplexed chip format? Are we, in fact, simply mimicking what Nature already exploits for long-range signaling among proteins in the cell that utilize DNA CT? Many more questions remain to be addressed, yet it is abundantly clear that DNA CT and, more specifically, DNA electrochemistry, represent a remarkably rich field for study.

REFERENCES

(1) Szent-Gyorgyi, A., Isenberg, I., Baird, S. L. (1960) *Proc. Natl. Acad. Sci. U. S. A. 46*, 1444–1449.

(2) Eley, D. D., Spivey, D. I. (1962) *Trans. Faraday Soc. 58*, 411–415.

(3) Boon, E. M., Barton, J. K. (2002) *Curr. Opin. Struc. Biol. 12*, 320–329.

(4) Delaney, S., Barton, J. K. (2003) *J. Org. Chem. 68*, 6475–6483.

(5) O'Neill, M. A., Barton, J. K. (2005) *Charge Transfer in DNA: From Mechanism to Application* (H.-A. Wagenknecht) pp. 27–75, Wiley–VCH, Hoboken.

(6) Giese, B. (2000) *Acc. Chem. Res. 33*, 631–636.

(7) Schuster, G. B. (2000) *Acc. Chem. Res. 33*, 253–260.

(8) Murphy, C. J., Arkin, M. R., Jenkins, Y., Ghatlia, N. D., Turro, N. J., Barton, J. K. (1993) *Science 262*, 1025–1029.

(9) Kelley, S. O., Holmlin, R. E., Stemp, E. D. A., Barton, J. K. (1997) *J. Am Chem. Soc. 119*, 9861–9870.

(10) Hall, D. B., Holmlin, R. E., Barton, J. K. (1996) *Nature 382*, 731–735.

(11) Nunez, M. E., Hall, D. B., Barton, J. K. (1999) *Chem. Biol. 6*, 85–97.

(12) Bhattacharya, P. K., Barton, J. K. (2001) *J. Am. Chem. Soc. 123*, 8649–8656.

(13) Williams, T. T., Dohno, C., Stemp, E. D. A., Barton, J. K. (2004) *J. Am. Chem. Soc. 126*, 8148–8158.

(14) Merino, E. J., Boal, A. K., Barton, J. K. (2008) *Curr. Opin. Chem. Biol. 12*, 229–237.

(15) Drummond, T. G., Hill, M. G., Barton, J. K. (2003) *Nature Biotechnol. 21*, 1192–1199.

(16) Bard, A. J., Faulkner, L. R. (2001) *Electrochemical Methods*, *2nd ed.*, John Wiley & Sons: New York.

(17) Love, J. C., Estroff, L. A., Kriebel, J. K., Nuzzo, R. G., Whitesides, G. M. (2005) *Chem. Rev. 105*, 1103–1169.

(18) Fink, H. W., Schonenberger, C. (1999) *Nature 398*, 407–410.

(19) Porath, D., Bezryadin, A., de Vries, S., Dekker, C. (2000) *Nature 403*, 635–638.

(20) Kasumov, A. Y., Kociak, M., Gueron, S., Reulet, B., Volkov, V. T., Klinov, D. V., Bouchiat, H. (2000) *Science 291*, 280–282.

(21) Guo, X., Gorodetsky, A. A., Hone, J., Barton, J. K., Nuckolls, C. (2008) *Nature Nanotechnol. 3*, 163–167.

(22) Kelley, S. O., Barton, J. K., Jackson, N. M., Hill, M. G. (1997) *Bioconjugate Chem. 8,* 31–37.

(23) Boon, E. M., Salas, J. E., Barton, J. K. (2002) *Nature Biotechnol. 20*, 282–286.

(24) Gore, M. R., Szalai, V. A., Ropp, P. A., Yang, I. V., Silverman, J. S., Thorp, H. H. (2003) *Anal. Chem. 75*, 6586–6592.

(25) Gorodetsky, A. A., Barton, J. K. (2006) *Langmuir 22*, 7917–7922.

(26) Rant, U., Arinaga, K., Fujita, S., Yokoyama, N., Abstreiter, G., Tornow, M. (2004) *Nano Lett. 4*, 2441–2445.

(27) Rant, U., Arinaga, K., Fujita, S., Yokoyama, N., Abstreiter, G., Tornow, M. (2004) *Langmuir 20*, 10086–10092.

(28) Arinaga, K., Rant, U., Tornow, M., Fujita, S., Abstreiter, G., Yokoyama, N. (2006) *Langmuir 22*, 5560–5562.

(29) Ceres, D. M., Barton, J. K. (2003) *J. Am. Chem. Soc. 125*, 14964–14965.

(30) Hihath, J., Xu, B., Zhang, P., Tao, N. (2005) *Proc. Natl. Acad. Sci. U. S. A. 102,* 16979–16983.

(31) Wierzbinski, E.; Arndt, J.; Hammond, W.; Slowinski, K. (2006) *Langmuir 22,* 2426–2429.

(32) Kelley, S. O., Barton, J. K., Jackson, N. M., McPherson, L. D., Potter, A. B., Spain, E. M., Allen, M. J., Hill, M. G. (1998) *Langmuir 14*, 6781–6784.

(33) Boon, E. M., Sam, M., Barton, J. K., Hill, M. G., Spain, E. M. (2001) *Langmuir 17*, 5727–5730.

(34) Zhou, D., Sinniah, K., Abell, C., Rayment, T. (2002) *Langmuir 18*, 8278–8281.

(35) Zhou, D., Sinniah, K., Abell, C., Rayment, T. (2003) *Angew. Chem. Int. Ed. 42*, 4394–4397.

(36) Erts, D., Polyakov, B., Olin, H., Tuite, E. (2003) *J. Phys. Chem. B. 107*, 3591–3597.

(37) Turcu, F., Schulte, A., Hartwich, G., Schuhmann, W. (2004) *Angew. Chem. Int. Ed. 43*, 3482–3485.

(38) Liu, B., Li, C.-Z., Kraatz, H.-B., Bard, A. J. (2005) *J. Phys. Chem. B. 109*, 5193–5198.

(39) Wain, A. J., Zhou, F. (2008) *Langmuir 24,* 5155–5160.

(40) Yang, X., Wang, Q., Wang, K., Tan, W., Yao, J., Li, H. (2006) *Langmuir 22*, 5654–5659.

(41) Li, Y.-J., Xiang, J., Zhou, F. (2007) *Plasmonics 2,* 79–87.

(42) Steel, A. B., Herne, T. M., Tarlov, M. J. (1998) *Anal. Chem. 70*, 4670–4677.

(43) Yu, H.-Z., Luo, C.-Y., Sankar, D. G., Sen, D. (2003) *Anal. Chem. 75*, 3902–3907.

(44) Ceres, D. M., Udit, A. K., Hill, H. D., Hill, M. G., Barton, J. K. (2007) *J. Phys. Chem. B. 111*, 663–668.

(45) Kelley, S. O., Boon, E. M., Barton, J. K., Jackson, N. M., Hill, M. G. (1999) *Nucl. Acids Res. 27*, 4830–4837.

(46) Boon, E. M., Ceres, D. M., Drummond, T. G., Hill, M. G., Barton, J. K. (2000) *Nature Biotechnol. 18*, 1096–1100.

(47) Boon, E. M., Jackson, N. M., Wightman, M. D., Kelley, S. O., Barton, J. K., Hill, M. G. (2003) *J. Phys. Chem. B 107*, 11805–11812.

(48) Boon, E. M., Barton, J. K., Bhagat, V., Nersissian, M., Wang, W., Hill, M. G. (2003) *Langmuir 19*, 9255–9259.

(49) Boal, A. K., Barton, J. K. (2005) *Bioconjugate Chem. 16*, 312–321.

(50) Kelley, S. O., Jackson, N. M., Hill, M. G., Barton, J. K. (1999) *Angew. Chem. Int. Ed. 38*, 941–945.

(51) Drummond, T. G., Hill, M. G., Barton, J. K. (2004) *J. Am. Chem. Soc. 126*, 15010–15011.

(52) Liu, T., Barton, J. K. (2005) *J. Am. Chem. Soc. 127*, 10160–10161.

(53) Gorodetsky, A. A., Barton, J. K. (2007) *J. Am. Chem. Soc. 129*, 6074–6075.

(54) Di Giusto, D. A., Wlasoff, W. A., Giesebrecht, S., Gooding, J. J., King, G. C. (2004) *J. Am. Chem. Soc. 126*, 4120–4121.

(55) Di Giusto, D. A., Wlasoff, W. A., Giesebrecht, S., Gooding, J. J., King, G. C. (2004) *Angew. Chem., Int. Ed. 116*, 2809–2812.

(56) Okamoto, A., Kamei, T., Tanaka, K., Saito, I. (2004) *J. Am. Chem. Soc.*, *126*, 14732–14733.

(57) Okamoto, A., Kamei, T., Saito, I. (2006) *J. Am. Chem. Soc. 128*, 658–662.

(58) Gorodetsky, A. A., Green, O., Yavin, E., Barton, J. K. (2007) *Bioconjugate Chem. 18*, 1434–1441.

(59) Gorodetsky, A. A., Dietrich, L. E. P., Lee, P. E. Demple, B., Newman, D. K., Barton, J. K. (2008) *Proc. Natl. Acad. Sci. U. S. A. 105*, 3684–3689.

(60) Gorodetsky, A. A., Ebrahim, A., Barton, J. K. (2008) *J. Am. Chem. Soc. 130*, 2924–2925.

(61) Gorodetsky, A. A., Hammond, W., Hill, M. G., Slowinski, K., Barton, J. K. (2008) *Langmuir ASAP.*

(62) Derosa, M. C., Sancar, A., Barton, J. K. (2005) *Proc. Natl. Acad. Sci. U. S. A. 102*, 10788–10792.

(63) David, S.S., Williams, S.D. (1998) *Chem. Rev. 98*, 1221–1262.

(64) Kuo, C. F., McRee, D. E., Fisher, C. L., O'Handley, S. F., Cunningham, R. P., Tainer, J. A. (1992) *Science 258*, 434–440.

(65) Thayer, M. M., Ahern, H., Xing, D., Cunningham, R. P., Tainer, J. A. (1995) *EMBO J. 14*, 4108–4120.

(66) Fromme, J. C., Verdine, G. L. (2003) *EMBO J. 22*, 3461–3471.

(67) Fromme, J. C., Banerjee, A., Huang, S. J., Verdine, G. L. (2004) *Nature 427*, 652–656.

(68) Porello, S. L., Cannon, M. J., David, S. S. (1998) *Biochemistry 37*, 6465–6475.

(69) Cunningham, R. P., Asahara, H., Bank, J. F., Scholes, C. P., Salerno, J. C., Surerus, K., Munck, E., McCracken, J., Peisach, J., Emptage, M. H. (1989) *Biochemistry 28*, 4450–4455.

(70) Fu, W., O'Handley, S., Cunningham, R. P., Johnson, M. K. (1992) *J. Biol. Chem. 267*, 16135–16137.

(71) Boon, E. M., Livingston, A. L., Chmiel, N. H., David, S. S., Barton, J. K. (2003) *Proc. Natl. Acad. Sci. U. S. A. 100*, 12543–12547.

(72) Boal, A. K., Yavin, E., Lukianova, O. A., O'Shea, V. L., David, S. S., Barton, J. K. (2005) *Biochemistry 44*, 8397–8407.

(73) Gorodetsky, A. A., Boal, A. K., Barton, J. K. (2006) *J. Am. Chem. Soc. 128*, 12082–12083.

(74) Pomposiello, P. J., Demple, B. (2001) *Trends Biotechnol. 19*, 109–114.

(75) Demple, B., Ding, H., Jorgensen, M. (2002) *Methods Enzymol. 348*, 355–364.

(76) Watanabe, S., Kita, A., Kobayashi, K., Miki, K. (2008) *Proc. Natl. Acad. Sci. U. S. A. 105*, 4121–4126.